

**Design rules for optimization of photophysical and kinetic properties of azoarene photoswitches**

Journal:	<i>Organic &amp; Biomolecular Chemistry</i>
Manuscript ID	OB-ART-08-2023-001298
Article Type:	Paper
Date Submitted by the Author:	21-Aug-2023
Complete List of Authors:	Adrion, Daniel; Northeastern University College of Science, Chemistry & Chemical Biology Lopez, Steven; Northeastern University College of Science, Chemistry & Chemical Biology;

Title: Design rules for optimization of photophysical and kinetic properties of azoarene photoswitches

Daniel M. Adrion and Steven A. Lopez\*

Department of Chemistry and Chemical Biology, Northeastern University, Boston, Massachusetts, 02115, United States

Corresponding author: [s.lopez@northeastern.edu](mailto:s.lopez@northeastern.edu)

### Abstract

Azoarenes are an important class of molecular photoswitches that often undergo  $E \rightarrow Z$  isomerization with ultraviolet light and have short  $Z$ -isomer lifetimes. Azobenzene has been a widely studied photoswitch for decades but can be poorly suited for photopharmacological applications due to its UV-light absorption and short-lived  $Z$ -isomer half-life ( $t_{1/2}$ ). Recently, diazo photoswitches with one or more thiophene rings in place of a phenyl ring have emerged as promising candidates, as they exhibit a stable photostationary state (98%  $E \rightarrow Z$  conversion) and  $E$ -isomer absorption ( $\lambda^{\max}$ ) in the visible light range (405 nm). In this work, we performed density functional theory calculations [PBE0-D3BJ/6-31+G(d,p)] on 26 *hemi*-azothiophenes, substituted with one phenyl ring and one thiophene ring on the diazo bond. We calculated the  $E$ -isomer absorption ( $\lambda^{\max}$ ) and  $Z$ -isomer  $t_{1/2}$  for a set of 26 *hemi*-azothiophenes. We compared their properties to thiophene-based photoswitches that have been studied previously. We separated the 26 proposed photoswitches into four quadrants based on their  $\lambda^{\max}$  and  $t_{1/2}$  relative to past generations of *hemi*-azothiophene photoswitches. We note 8 *hemi*-azothiophenes with redshifted  $\lambda^{\max}$  and longer  $t_{1/2}$  than previous systems. Our top candidate has  $\lambda^{\max}$  and a  $t_{1/2}$  approaching 360 nm and 279 years, respectively. The results here present a pathway towards leveraging and optimizing two properties of photoswitches previously thought to be inversely related.

### Introduction

Azobenzene is the prototypical photoswitch; its photophysical and energy-storing properties are well-known, and it can be readily synthesized.<sup>1-7</sup> Azoarenes have been used for applications in materials science<sup>8-12</sup> and photopharmacology.<sup>13-15</sup> Azoarene photoswitches are a general class of azobenzene derivatives that offer considerable structural diversity and undergo light-promoted  $E \rightarrow Z$  isomerization when irradiated with ultraviolet to infrared light.<sup>9, 16-18</sup> Recent efforts in the field have focused on heteroarenes such as pyrazoles<sup>19-23</sup> and thiophenes,<sup>24-26</sup> because of their red-shifted absorption maximum ( $\lambda^{\max}$ ) and promising band separation in the  $E$ - and  $Z$ -isomers. There has been a broad effort to red-shift the absorption maximum ( $\lambda^{\max}$ ) of the azobenzene  $E$ -isomer ( $\lambda^{\max} = 320$  nm) into the visible-light range to minimize photodamage in living organisms.<sup>27, 28</sup> This is especially true in photopharmacology, where the half-life ( $t_{1/2}$ ) of the metastable  $Z$ -isomer needs to be on the order of days to establish a stable photostationary state.<sup>17</sup> In 2019, Fuchter and co-workers synthesized a series of *hemi*-azopyrazole photoswitches showing UV-promoted photoswitching (80-93%  $Z$ -isomer population) and long-lived  $Z$ -isomer  $t_{1/2}$  (up to 46 years).<sup>29</sup> In 2021, a set of *bis*-azopyrazoles discovered by Li and co-workers exhibited nearly complete  $E \rightarrow Z$  photoconversion (94-98%) and a  $Z$ -isomer  $t_{1/2}$  of up to 681 days.<sup>22</sup> Our group recently reported the results of a high-throughput virtual screening (HTVS) where we observed significant differences in the  $\lambda^{\max}$  and  $t_{1/2}$  values for a set of positional isomers of *bis*-azofurans and *bis*-azothiophenes.<sup>30</sup> We showed that isomeric *bis*-azothiophenes and *bis*-diazofurans (2,2 vs. 3,3) increased the  $\lambda^{\max}$  of the  $E$ -

isomers by as much as 77 nm while simultaneously lowering the  $t_{1/2}$  by six orders of magnitude. These changes resulted from the cross-conjugation vs.  $\pi$ -conjugation significantly increasing the activation free energies ( $\Delta G^\ddagger$ ) and shorter  $\lambda^{\max}$  wavelengths for the (3,3) isomers.

Wegner and Heindl showed that the  $\lambda^{\max}$  and  $t_{1/2}$  of *hemi*-2-thiophenes with a phenyl terminus can be tuned through functionalization on both aryl rings.<sup>25</sup> They synthesized a series of azothiophenes with substituents on the *meta* and *para* positions on the phenyl ring and at the 5-position on the thiophene ring. They determined the *E*-isomer  $\lambda^{\max}$  and *Z*-isomer  $t_{1/2}$  for each. They reported  $\lambda^{\max}$  values approaching 405 nm (through substitution of the thiophene ring with a methoxy group) and high (>99%) *E*  $\rightarrow$  *Z* photoconversion efficiencies (through substitution of the phenyl ring at the *meta* position with a CN functional group). Although the 2-*hemi*-thiophenes displayed red-shifted *E*-isomer  $\lambda^{\max}$  values ranging from 45-85 nm compared to azobenzene, the  $t_{1/2}$  lifetimes were shorter (maximum  $t_{1/2}$  of 17.7 hours) than those of azobenzene (2 days in CH<sub>3</sub>CN).

Past experimental and computational work on azoarenes has shown an empirical inverse relationship between the  $\lambda^{\max}$  and  $t_{1/2}$ .<sup>17, 20, 31</sup> This leads to trade-offs during photoswitch design. This report describes how we have applied strategies to increase the  $\lambda^{\max}$  and  $t_{1/2}$  metrics to design photoswitches *a priori* for photopharmacological applications. We designed a new class of *hemi*-azothiophenes with the diazo group bound to a *p*-substituted-phenyl and thiophene substituted at the 3-position. This photoswitch was designed to maximize  $t_{1/2}$  based on our recent discovery of the role of cross-conjugation on (3,3)-vs. (2,2)-*bis*-azothiophenes and similar experimental reports by Perry and co-workers.<sup>26</sup> We combined this powerful effect with known strategies to simultaneously increase  $\lambda^{\max}$  (i.e., increasing  $\pi$ -conjugation length and substituent effects). To this end, we computed the  $\lambda^{\max}$  and  $t_{1/2}$  of 26 *hemi*-azothiophenes with quantum mechanical density functional theory calculations, enabled by our automated computational workflow, *EZ*-TS.<sup>32</sup>

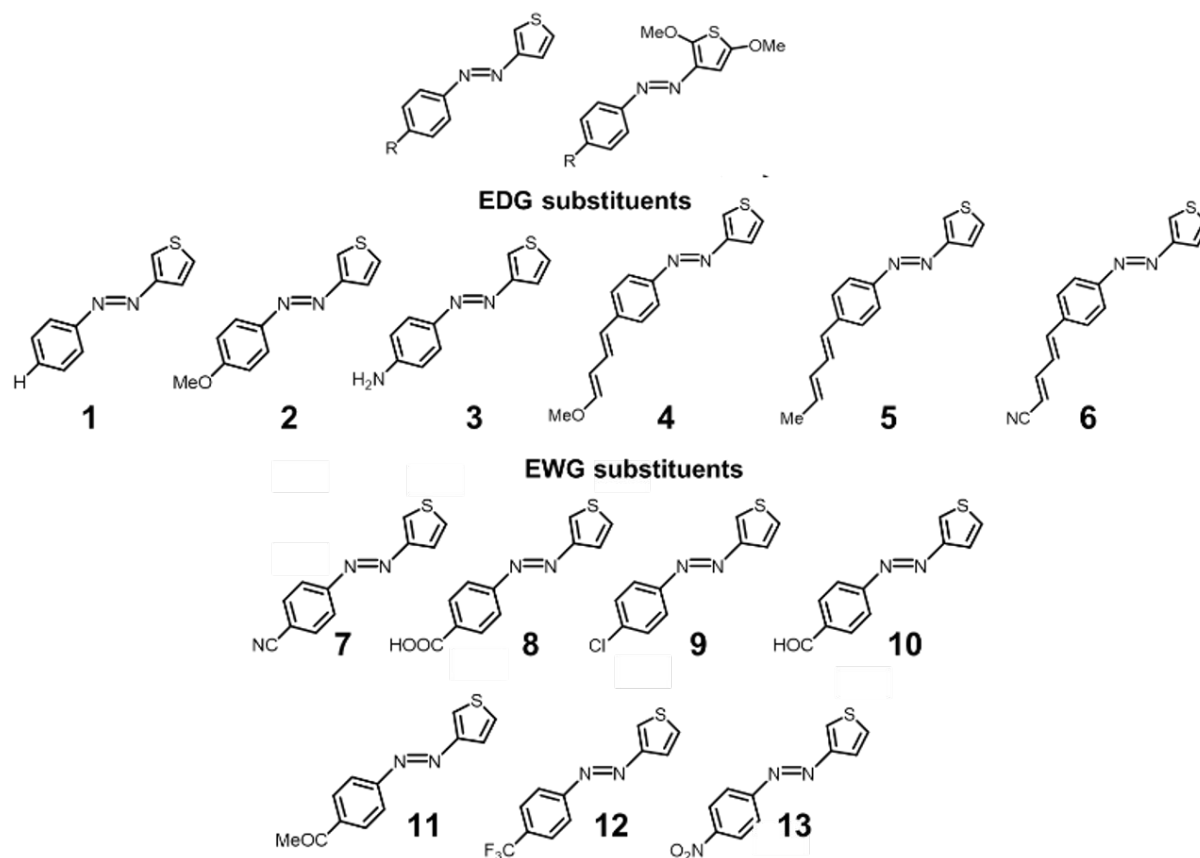
The *EZ*-TS code first generates a set of 12 transition state guesses from an input *Z*-isomer geometry by rotating about the diazo bond. The 12 guess structures are optimized using B3LYP-D3BJ/6-31G(d), and the lowest energy guess structure is subject to a conformational analysis with the Conformer Rotamer Ensemble Sampling Tool (CREST).<sup>33</sup> Next, a 5-step constrained relaxation using ORCA<sup>34</sup> is run on all conformers to ensure a smooth convergence for the final set of optimizations and frequency calculations, which are performed on the 10 lowest energy conformers using B3LYP-D3BJ/6-31G(d).<sup>35-38</sup> At the end of this final step, the 10 conformers are ranked by their energies. The lowest energy conformer with a vibrational frequency corresponding to the *Z*  $\rightarrow$  *E* thermal isomerization reaction is determined to be the lowest energy transition state. We benchmarked this workflow for 11 azoarenes and 140 model chemistries. We found that the PBE0-D3BJ<sup>39</sup> with either the cc-pVDZ<sup>40, 41</sup> or 6-31+G(d,p)<sup>35</sup> basis sets provide the best balance between computational cost and accuracy; the mean absolute error (MAE) for this model chemistry was 1.3 kcal mol<sup>-1</sup>. This was the first comprehensive study that benchmarked DFT model chemistries for their accuracy in computing *Z*  $\rightarrow$  *E* thermal isomerization barriers for azoarenes.

Past studies on the thermal mechanisms of azoarene photoswitches have determined three possible mechanisms for the *Z*  $\rightarrow$  *E* isomerization reaction. These include rotation about the CNNC dihedral,<sup>22, 42, 43</sup> inversion of the  $\pi_{\text{NN}}$  bond, and a hula-twist mechanism where there is a twisting motion about the  $\pi$ -bond, and the aryl groups maintain their relative orientations.<sup>44</sup> Past experimental and computational work on azoarenes shows a preference for the inversion

mechanism. Because the 3-substituted photoswitches significantly increase the  $t_{1/2}$ , we chose to study these further.

Scheme 1 shows all 26 azoarenes included in this study. We present 13 with an unsubstituted thiophene ring and 13 with 2,5-dimethoxy thiophenes. We substituted methoxy groups on the thiophene because Wegner observed longer  $t_{1/2}$  values for azothiophenes with EDGs substituted at the 4-position.

**Scheme 1.** Parent structure for *hemi*-azothiophene and substituted *hemi*-azothiophene photoswitches tested for this work.



We hypothesize that adding  $\pi$ -donating groups (OMe) on the thiophene will red-shift the otherwise low *E*-isomer  $\lambda^{\max}$  value for 3-substituted *hemi*-azothiophenes. We used a combination of electron donating groups (EDGs), including  $\text{NH}_2$ , OMe, and three vinyl dienes with OMe, Me, and CN terminal groups (Scheme 1). We also used seven electron-withdrawing groups (EWGs), including  $\text{NO}_2$ ,  $\text{CF}_3$ , CN, COOH, COH, COMe, and Cl. Through aryl ring functionalization, we aim to find an optimal thiophene photoswitch with red-shifted  $\lambda^{\max}$  and longer  $t_{1/2}$  lifetimes than previously studied generation of *hemi*-azothiophene photoswitches.

## Results and Discussion

All transition structure calculations were performed in Gaussian 16<sup>45</sup> with the PBE0-D3BJ/6-31+G(d,p) method and the IEFPCM<sup>water</sup> solvation model,<sup>46</sup> which we found to have an optimal balance of accuracy and computational cost.<sup>32</sup> Next, we performed intrinsic reaction coordinate (IRC) calculations and optimized the reactive conformers corresponding to the *E* and *Z* isomers for a given thermal isomerization. The reactive *Z*-

isomers were used to calculate the thermal barrier. For our set of 26 photoswitches, we confirmed that 17 underwent an inversion mechanism, while the remaining 9 underwent rotation. All systems that underwent a rotation mechanism were substituted with OMe groups on the thiophene ring, while all photoswitches with unsubstituted thiophene rings underwent an inversion mechanism. All transition state geometries are given in the supporting information (SI).

The range of computed  $\Delta G^\ddagger$  for was found to be 16.5 kcal mol<sup>-1</sup>, corresponding to  $t_{1/2}$  values ranging from 10<sup>-3</sup> seconds to 10<sup>5</sup> years (nearly 12 orders of magnitude). Figure 1 shows the transition state geometries for systems with the smallest and largest  $t_{1/2}$  values for the unsubstituted and substituted thiophene rings, respectively. The shortest lifetime was for the systems with the nitro-substituted phenyl ring, and the longest lifetime was for the systems with an amine substituent on the phenyl ring.

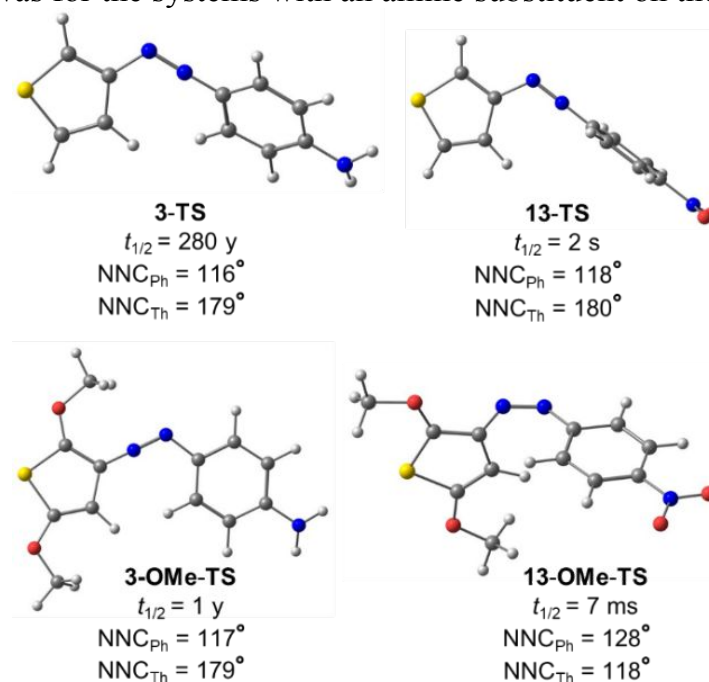


**Figure 1.** Transition state geometries corresponding to the systems with highest and lowest  $t_{1/2}$  for the unsubstituted thiophenes (top) and methoxy substituted systems (bottom).  $\text{NNC}_{\text{Ph}}$  corresponds to the angle with the carbon atom in the phenyl ring, and  $\text{NNC}_{\text{Th}}$  corresponds to the angle including the carbon atom on the thiophene rings.

Figure 1 shows the computed transition structures and  $t_{1/2}$  for **3-TS**, **13-TS**, **3-OMe-TS**, and **13-OMe-TS**, representing the strongest EWG- and EDG-substituents (NH<sub>2</sub> vs. NO<sub>2</sub>, respectively). Our calculations show approximately 10 orders of magnitude difference in  $t_{1/2}$ . This increase in  $t_{1/2}$  is observed for both the unsubstituted thiophene (**3-TS** and **13-TS**) and 2,5-dimethoxythiophenes (**3-OMe-TS** and **13-OMe-TS**). Three of the four *hemi*-azothiophenes in Figure 1 undergo inversion mechanisms (**3**, **13**, and **3-OMe**), while **13-OMe-TS** isomerizes through a rotation mechanism. Different NNC angles about the diazo bond characterize these mechanisms. For the inversion mechanism, one of the NNC angles is linear, whereas the other is nearly 120° (116° - 118°). The rotation transition structures do not have a linear CNN angle about the diazo (128° and 118° for **13-OMe-TS** for  $\text{NNC}_{\text{Ph}}$  and  $\text{NNC}_{\text{Th}}$ , respectively). We assessed the role of the EDGs and EWGs in delocalizing  $\pi_{\text{NN}}$ -electrons to explain the nearly 12 orders of magnitude range in  $t_{1/2}$  for **1-13** and **(1-13)-OMe**. We plotted the  $\Delta G^\ddagger$  for 20 of the 26 photoswitches against the Hammett ( $\sigma_{\text{para}}$ ) parameters (there are no reported

$\sigma_{\text{para}}$  values for the methoxy diene groups in **11-13** and **(11-13)-OMe**. The Hammett parameter quantifies how much a given functional group stabilizes a developing negative charge in a transition structure. Venkataramani and König showed that azoarene  $Z \rightarrow E$  thermal isomerization barriers decrease with the strength of EWGs at *para*-Ph positions.<sup>20, 21</sup>

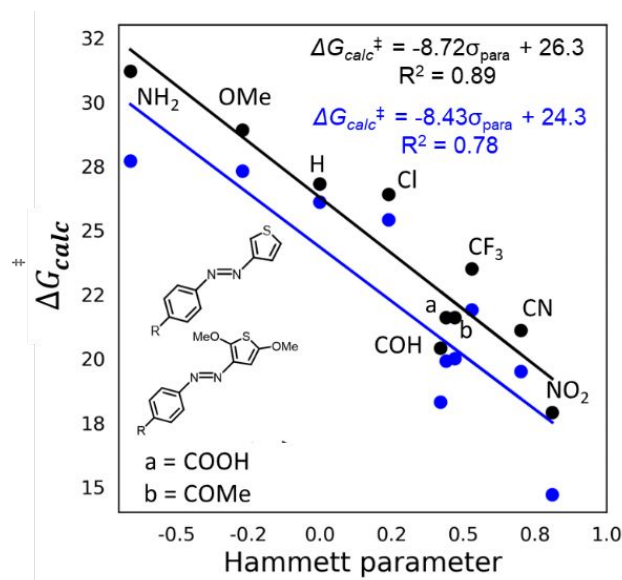


**Figure 2.** Scatterplot showing the relationship between Hammett parameter  $\sigma_{\text{para}}$  and calculated activation barrier for unsubstituted (black) and dimethoxy (blue) *hemi*-thiophene systems. The linear correlation equation and  $R^2$  are presented. The barriers are shown in kcal mol<sup>-1</sup>. The “a” and “b” groups correspond to the carboxylic acid and ketone groups, respectively.

Figure 2 shows the linear relationship between the calculated ( $\Delta G^{\ddagger}$ ) and  $\sigma_{\text{para}}$  for **1-3** and **7-13** (black line), and **(1-3)-OMe** and **(7-13)-OMe** (blue line). We used a broad range of EWG- and EDG-substituents ( $\sigma_{\text{para}}$  ranges from -0.66 – 0.81). The  $R^2$  values are 0.89 and 0.78 for the unsubstituted and dimethoxy-thiophenes, respectively. The linear correlation suggests there is a moderately strong relationship between the ability of a substituent to delocalize the  $\pi_{\text{NN}}$ -electrons and the  $\Delta G^{\ddagger}$ . The slopes are -8.72 (black line) and -8.43 (blue line), which indicate that the unsubstituted thiophenes (**1-13**) are slightly more sensitive to the substituent effects than the 2,5-dimethoxy thiophenes [**(1-13)-OMe**]. We present our computed results for all 26 *hemi*-azothiophenes in the scatterplot in Figure 3. We compared our computed  $\lambda^{\text{max}}$  and  $t_{1/2}$  to those of *hemi*-azothiophene reported by Wegner in 2020 ( $\lambda^{\text{max}}$  of 365 nm and  $t_{1/2}$  of 17.7 hours).<sup>47</sup> The scatterplot is organized into four quadrants; The red quadrant (bottom left) contains photoswitches where both  $\lambda^{\text{max}}$  and  $t_{1/2}$  are lower relative to the past system, while the yellow quadrants (top left and bottom right) have a red-shifted  $\lambda^{\text{max}}$  and shorter  $t_{1/2}$  (top-left) or a longer  $t_{1/2}$  and a lower  $\lambda^{\text{max}}$  (bottom right) compared to the past system. The green quadrant (top right) contains eight photoswitches from our set with red-shifted  $\lambda^{\text{max}}$  and longer  $t_{1/2}$  than *hemi*-azothiophene.

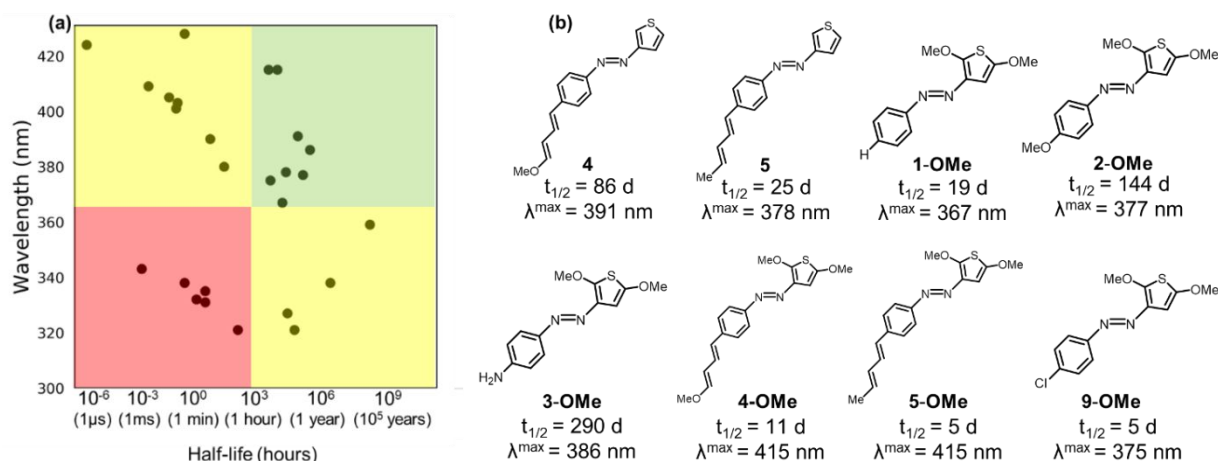


**Figure 3.** Scatterplot showing 26 thermal *Z/E* isomerization  $t_{1/2}$  plotted against the *E*-isomer  $\lambda_{\max}$  (4a). The eight azothiophenes in the green quadrant are presented (4b). The  $\lambda_{\max}$  values were computed using  $\omega$ b97-XD/aug-cc-pVTZ and IEFPCM<sup>water</sup>, and the  $t_{1/2}$  were calculated using PBE0-D3BJ/6-31+G(d,p) and IEFPCM<sup>water</sup>.

There are six *hemi*-azothiophenes contained in the red quadrant of the scatter plot in Figure 3. All six of these structures have a lower  $\lambda_{\max}$  and shorter  $t_{1/2}$  than unsubstituted *hemi*-azothiophene (365 nm and 17.7 hours, respectively). The six photoswitches are 7, 8, 9, 10, 11, and 12, and are all substituted with EWGs (CN, COOH, COH, COMe, CF<sub>3</sub>, and NO<sub>2</sub>, respectively) at the phenyl ring *para*-position. These results and figure 2 in the main body of the manuscript suggest that substituting the phenyl ring with an EWG will significantly lower the *Z*-isomer  $t_{1/2}$  of the *hemi*-azothiophene photoswitches; the energy of the transition state is lowered due to resonance stabilization from a strong EWG (the Hammett plot to show this trend is shown in figure 2 of the manuscript). *Hemi*-azothiophenes 7-12 from the paper also have an unsubstituted thiophene ring bonded to the diazo bond, which suggests that functionalizing the thiophene in *hemi*-azothiophene red shifts  $\lambda_{\max}$ .

The eight molecules (4, 5, 1-OMe, 2-OMe, 3-OMe, 5-OMe, 6-OMe, and 9-OMe) in Figure 3b have computed  $\lambda_{\max}$  values that range from 367-415 nm and  $t_{1/2}$  values that range from 5-290 days. Six of the eight photoswitches (4, 5, 2-OMe, 3-OMe, 4-OMe, and 5-OMe) are substituted with an EDG at the *para* position on the phenyl ring, which increased the  $\lambda_{\max}$  compared to an unsubstituted or EWG-substituted Ph group. 1-OMe has the lowest  $\lambda_{\max}$  (367 nm) of the eight photoswitches in the green quadrant. Six of the eight photoswitches in the green quadrant are substituted on the thiophene ring with methoxy groups, consistent with EDGs red shifting the  $\lambda_{\max}$  of azoarene photoswitches. We also observed that extending  $\pi$ -conjugation through a methoxy diene group significantly red-shifted the  $\lambda_{\max}$  of the photoswitches while maintaining a relatively long-lived  $t_{1/2}$  (as seen in 4, 5, and (4-5)-OMe). Our results show that all methoxy-substituted azothiophenes have lower  $\Delta G^\ddagger$  than unsubstituted thiophene rings (barriers decreased by 0.6 – 3.5 kcal mol<sup>-1</sup>) while significantly increasing the  $\lambda_{\max}$  (an increase of 24 – 81 nm for the *E*-isomer). Due to the cross-conjugation of the thiophene ring, the dimethoxy-substituted photoswitches offer red-shifted  $\lambda_{\max}$  and longer  $t_{1/2}$  over previously reported azothiophenes.

## Conclusion

We have used quantum chemical calculations (TDDFT and DFT) to calculate the vertical excitation energies and  $t_{1/2}$  of a set of 26 *hemi*-thiophene photoswitches. Our findings suggest it is possible to optimize these properties, generally considered to possess an inverse relationship, simultaneously. The 26 azoarenes have a  $t_{1/2}$  range of nearly 12 orders of

magnitude ( $10^{-3}$  seconds to  $10^5$  years), and an *E*-isomer  $\lambda^{\max}$  range of 107 nm (321 – 428 nm). We have also established a relationship between the Hammett parameters ( $\sigma_{\text{para}}$ ) and the calculated thermal barriers for 20 *hemi*-azothiophene systems. We found that EWGs lower the energy of the TS geometry through the delocalization of the  $\pi$ -NN electrons. We are collaborating with experimentalists to validate these design principles and produce azoarenes of interest to photopharmacology.

### Computational methods

We used DFT calculations to predict the activation free energies ( $\Delta G^\ddagger$ ) and vertical excitation energies of **1–13** and **1-OMe–13-OMe**. We computed the structures and energies of the *Z*-isomers, *E*-isomers, and transition structures for the 26 *hemi*-azothiophene isomerization reactions. After optimizing the transition state structures, we ran intrinsic reaction coordinate (IRC) calculations and optimized the endpoints corresponding to the *E* and *Z*-isomer reactive conformers. All calculations were performed using the Gaussian 16 software. We used the PBE0-D3BJ/6-31+G(d,p) model chemistry for the geometry optimizations and subsequent vibrational frequency calculations. Vertical excitation energies for all systems were calculated using TD-DFT with the  $\omega$ B97X-D/6-311+G(d,p) model chemistry in IEFPCM<sup>water</sup>. The lowest 10 singlet states were included in all TD-DFT calculations. The  $\Delta G^\ddagger$  values presented in kcal mol<sup>-1</sup> were converted to  $t_{1/2}$  (units of seconds) by using the Eyring equation at room temperature (293.15 K).

### Conflicts of interest

The authors declare no conflicts of interest.

### Acknowledgments

D. M. A. and S.A.L. acknowledge the National Science Foundation CAREER award (NSF-CHE-2144556) and Camille Dreyfus Teacher-Scholar Award for funding. All authors appreciate the assistance from the Northeastern Research Computing Team and the computing resources provided by the Massachusetts Life Science Center grant (G00006360).

### References

1. Wang, Y.; Xie, R.; Huang, L.; Tian, Y.-N.; Lv, S.; Kong, X.; Li, S., Divergent synthesis of unsymmetrical azobenzenes via Cu-catalyzed C–N coupling. *Org. Chem. Front.* **2021**, *8* (21), 5962-5967.
2. Staubitz, A.; Walther, M.; Kipke, W.; Schultzke, S.; Ghosh, S., Modification of Azobenzenes by Cross-Coupling Reactions. *Synthesis* **2021**, *53* (07), 1213-1228.
3. Heindl, A. H.; Wegner, H. A., Starazo triple switches - synthesis of unsymmetrical 1,3,5-tris(aryloxy)benzenes. *Beilstein J Org Chem* **2020**, *16*, 22-31.
4. Feringa, B. L., *Molecular Switches*. Wiley - VCH: 2001.
5. Hamon, F.; Djedaini-Pillard, F.; Barbot, F.; Len, C., Azobenzenes—synthesis and carbohydrate applications. *Tetrahedron* **2009**, *65* (49), 10105-10123.
6. Merino, E.; Ribagorda, M., Control over molecular motion using the cis-trans photoisomerization of the azo group. *Beilstein J Org Chem* **2012**, *8*, 1071-90.
7. Merino, E., Synthesis of azobenzenes: the coloured pieces of molecular materials. *Chem Soc Rev* **2011**, *40* (7), 3835-53.
8. Martinez-Lopez, D.; Babalhavaeji, A.; Sampedro, D.; Woolley, G. A., Synthesis and characterization of bis(4-amino-2-bromo-6-methoxy)azobenzene derivatives. *Beilstein J Org Chem* **2019**, *15*, 3000-3008.
9. Lameijer, L. N.; Budzak, S.; Simeth, N. A.; Hansen, M. J.; Feringa, B. L.; Jacquemin, D.; Szymanski, W., General Principles for the Design of Visible-Light-

- Responsive Photoswitches: Tetra-ortho-Chloro-Azobenzenes. *Angew Chem Int Ed Engl* **2020**, *59* (48), 21663-21670.
10. Dumur, F., Recent advances on visible light Thiophene-based photoinitiators of polymerization. *Eur. Polym. J.* **2022**, *169*.
  11. Fernandes, R. S.; Shetty, N. S.; Mahesha, P.; Gaonkar, S. L., A Comprehensive Review on Thiophene Based Chemosensors. *J Fluoresc* **2022**, *32* (1), 19-56.
  12. Leistner, A. L.; Pianowski, Z. L., Smart Photochromic Materials Triggered with Visible Light. *Eur. JOC* **2022**, *2022* (19).
  13. Morstein, J.; Trauner, D., Photopharmacological control of lipid function. *Methods Enzymol* **2020**, *638*, 219-232.
  14. Doroudgar, M.; Morstein, J.; Becker-Baldus, J.; Trauner, D.; Glaubitz, C., How Photoswitchable Lipids Affect the Order and Dynamics of Lipid Bilayers and Embedded Proteins. *J Am Chem Soc* **2021**, *143* (25), 9515-9528.
  15. Cheng, B.; Morstein, J.; Ladefoged, L. K.; Maesen, J. B.; Schiott, B.; Sinning, S.; Trauner, D., A Photoswitchable Inhibitor of the Human Serotonin Transporter. *ACS Chem Neurosci* **2020**, *11* (9), 1231-1237.
  16. Hansen, M. J.; Lerch, M. M.; Szymanski, W.; Feringa, B. L., Direct and Versatile Synthesis of Red-Shifted Azobenzenes. *Angew Chem Int Ed Engl* **2016**, *55* (43), 13514-13518.
  17. Konrad, D. B.; Savasci, G.; Allmendinger, L.; Trauner, D.; Ochsenfeld, C.; Ali, A. M., Computational Design and Synthesis of a Deeply Red-Shifted and Bistable Azobenzene. *J Am Chem Soc* **2020**, *142* (14), 6538-6547.
  18. Dong, M.; Babalhavaeji, A.; Collins, C. V.; Jarrah, K.; Sadovski, O.; Dai, Q.; Woolley, G. A., Near-Infrared Photoswitching of Azobenzenes under Physiological Conditions. *J Am Chem Soc* **2017**, *139* (38), 13483-13486.
  19. Weston, C. E.; Richardson, R. D.; Haycock, P. R.; White, A. J.; Fuchter, M. J., Arylazopyrazoles: azoheteroarene photoswitches offering quantitative isomerization and long thermal half-lives. *J Am Chem Soc* **2014**, *136* (34), 11878-81.
  20. Devi, S.; Saraswat, M.; Grewal, S.; Venkataramani, S., Evaluation of Substituent Effect in Z-Isomer Stability of Arylazo-1 H-3,5-dimethylpyrazoles: Interplay of Steric, Electronic Effects and Hydrogen Bonding. *J Org Chem* **2018**, *83* (8), 4307-4322.
  21. Rustler, K.; Nitschke, P.; Zahnbrecher, S.; Zach, J.; Crespi, S.; Konig, B., Photochromic Evaluation of 3(5)-Arylazo-1H-pyrazoles. *J Org Chem* **2020**, *85* (6), 4079-4088.
  22. He, Y.; Shangguan, Z.; Zhang, Z. Y.; Xie, M.; Yu, C.; Li, T., Azobispyrazole Family as Photoswitches Combining (Near-) Quantitative Bidirectional Isomerization and Widely Tunable Thermal Half-Lives from Hours to Years\*. *Angew Chem Int Ed Engl* **2021**, *60* (30), 16539-16546.
  23. Simke, J.; Bosking, T.; Ravoo, B. J., Photoswitching of ortho-Aminated Arylazopyrazoles with Red Light. *Org Lett* **2021**, *23* (19), 7635-7639.
  24. Slavov, C.; Yang, C.; Heindl, A. H.; Wegner, H. A.; Dreuw, A.; Wachtveitl, J., Thiophenylazobenzene: An Alternative Photoisomerization Controlled by Lone-Pairpi Interaction. *Angew Chem Int Ed Engl* **2020**, *59* (1), 380-387.
  25. Wegner, A. H. H. a. H. A., Rational Design of Azothiophenes - Substituted Effects on the Switching Properties. *Chem. Eur. J.* **2020**, *26* (60), 13730-13737.
  26. Huddleston, P. R.; Volkov, V. V.; Perry, C. C., The structural and electronic properties of 3,3'-azothiophene photo-switching systems. *Phys Chem Chem Phys* **2019**, *21* (3), 1344-1353.
  27. Frangioni, J. V., In vivo near-infrared fluorescence imaging. *Curr Opin Chem Biol* **2003**, *7* (5), 626-34.
  28. Weissleder, R., A clearer vision for *in vivo* imaging. *Nat. Biotechnol.* **2001**, *19*, 316-317.
  29. Calbo, J.; Thawani, A. R.; Gibson, R. S. L.; White, A. J. P.; Fuchter, M. J., A combinatorial approach to improving the performance of azoarene photoswitches. *Beilstein J Org Chem* **2019**, *15*, 2753-2764.

30. Adrion, D. M.; Lopez, S. A., Cross-conjugation controls the stabilities and photophysical properties of heteroazoarene photoswitches. *Org Biomol Chem* **2022**, *20* (30), 5989-5998.
31. Zhang, Z. Y.; He, Y.; Zhou, Y.; Yu, C.; Han, L.; Li, T., Pyrazolylazophenyl Ether-Based Photoswitches: Facile Synthesis, (Near-)Quantitative Photoconversion, Long Thermal Half-Life, Easy Functionalization, and Versatile Applications in Light-Responsive Systems. *Chemistry* **2019**, *25* (58), 13402-13410.
32. Adrion, D. M.; Kaliakin, D. S.; Neal, P.; Lopez, S. A., Benchmarking of Density Functionals for Z-Azoarene Half-Lives via Automated Transition State Search. *J. Phys. Chem. A* **2021**, *125* (29), 6474-6485.
33. Pracht, P.; Bohle, F.; Grimme, S., Automated exploration of the low-energy chemical space with fast quantum chemical methods. *Phys Chem Chem Phys* **2020**, *22* (14), 7169-7192.
34. Neese, F., The ORCA program system. *WIREs Comp. Mol. Sci.* **2011**, *2* (1), 73-78.
35. Ditchfield, R.; Hehre, W. J.; Pople, J. A., Self-Consistent Molecular-Orbital Methods. IX. An Extended Gaussian-Type Basis for Molecular-Orbital Studies of Organic Molecules. *J. Chem. Phys.* **1971**, *54* (2), 724-728.
36. Becke, A. D., Density-functional thermochemistry. III. The role of exact exchange. *J. Chem. Phys.* **1993**, *98* (7), 5648-5652.
37. Lee, C.; Yang, W.; Parr, R. G., Development of the Colle-Salvetti correlation-energy formula into a functional of the electron density. *Phys Rev B Condens Matter* **1988**, *37* (2), 785-789.
38. Vosko, S. H.; Wilk, L.; Nusair, M., Accurate spin-dependent electron liquid correlation energies for local spin density calculations: a critical analysis. *Can. J. Phys.* **1980**, *58* (8), 1200-1211.
39. Adamo, C.; Barone, V., Toward reliable density functional methods without adjustable parameters: The PBE0 model. *J. Chem. Phys.* **1999**, *110* (13), 6158-6170.
40. Kendall, R. A.; Dunning, T. H.; Harrison, R. J., Electron affinities of the first-row atoms revisited. Systematic basis sets and wave functions. *J. Chem. Phys.* **1992**, *96* (9), 6796-6806.
41. Woon, D. E.; Dunning, T. H., Gaussian basis sets for use in correlated molecular calculations. V. Core-valence basis sets for boron through neon. *J. Chem. Phys.* **1995**, *103* (11), 4572-4585.
42. Crecca, C. R.; Roitberg, A. E., Theoretical study of the isomerization mechanism of azobenzene and disubstituted azobenzene derivatives. *J Phys Chem A* **2006**, *110* (26), 8188-203.
43. Gagliardi, L.; Orlandi, G.; Bernardi, F.; Cembran, A.; Garavelli, M., A theoretical study of the lowest electronic states of azobenzene: the role of torsion coordinate in the cis-trans photoisomerization. *Theo. Chem. Acc.* **2003**, *111* (2-6), 363-372.
44. Muzdalo, A.; Saalfrank, P.; Vreede, J.; Santer, M., Cis-to- Trans Isomerization of Azobenzene Derivatives Studied with Transition Path Sampling and Quantum Mechanical/Molecular Mechanical Molecular Dynamics. *J. Chem. Theory. Comput.* **2018**, *14* (4), 2042-2051.
45. Frisch, M. J.; Trucks, G. W.; Schlegel, H. B.; Scuseria, G. E.; Robb, M. A.; Cheeseman, J. R.; Scalmani, G.; Barone, V.; Petersson, G. A.; Nakatsuji, H.; Li, X.; Caricato, M.; Marenich, A. V.; Bloino, J.; Janesko, B. G.; Gomperts, R.; Mennucci, B.; Hratchian, H. P.; Ortiz, J. V.; Izmaylov, A. F.; Sonnenberg, J. L.; Williams; Ding, F.; Lipparini, F.; Egidi, F.; Goings, J.; Peng, B.; Petrone, A.; Henderson, T.; Ranasinghe, D.; Zakrzewski, V. G.; Gao, J.; Rega, N.; Zheng, G.; Liang, W.; Hada, M.; Ehara, M.; Toyota, K.; Fukuda, R.; Hasegawa, J.; Ishida, M.; Nakajima, T.; Honda, Y.; Kitao, O.; Nakai, H.; Vreven, T.; Throssell, K.; Montgomery Jr., J. A.; Peralta, J. E.; Ogliaro, F.; Bearpark, M. J.; Heyd, J. J.; Brothers, E. N.; Kudin, K. N.; Staroverov, V. N.; Keith, T. A.; Kobayashi, R.; Normand, J.; Raghavachari, K.; Rendell, A. P.; Burant, J. C.; Iyengar, S. S.; Tomasi, J.; Cossi, M.; Millam, J. M.; Klene, M.; Adamo, C.; Cammi, R.; Ochterski, J.

W.; Martin, R. L.; Morokuma, K.; Farkas, O.; Foresman, J. B.; Fox, D. J. *Gaussian 16 Rev. C.01*, Wallingford, CT, 2016.

46. Tomasi, J.; Mennucci, B.; Cammi, R., Quantum mechanical continuum solvation models. *Chem. Rev.* **2005**, *105* (8), 2999-3093.

47. Heindl, A. H.; Wegner, H. A., Rational Design of Azothiophenes-Substitution Effects on the Switching Properties. *Chemistry* **2020**, *26* (60), 13730-13737.